PDLC films for control of light transmission

1994 J. Phys. D: Appl. Phys. 27 2145

(http://iopscience.iop.org/0022-3727/27/10/023)

J. Phys. D: Appl. Phys. 27 (1994) 2145–2151. Printed in the UK

PDLC films for control of light transmission

W Körner, H Scheller, A Beck and J Fricke

Physikalisches Institut der Universität, Am Hubland, 97074 Würzburg, Germany

Received 26 July 1993, in final form 25 July 1994

Abstract. We have investigated the light switching properties of polymer dispersed liquid crystal (PDLC) films, which can be characterized by the spectral change in transmittance and reflectance due to switching by application of a suitable electrical voltage. The PDLC samples were prepared using the standard liquid crystal mixture E7 in a UV-curable matrix material. Using these samples, a transmission reduction of up to 30% was achieved in the solar spectral range. A strong dependence of the light switching behaviour on the mass ratio of liquid crystal and matrix material as well as on the curing rate of the matrix material was found, whereas the film thickness has only a small influence. Light scattering measurements allowed us to determine the average size of the scattering centres. In the samples investigated the liquid crystal droplets have radii below 2 μm. Additional measurements of the electric properties of the PDLC films showed that the capacity and the resistivity of the PDLC films depend on both the applied AC voltage and its frequency. The power consumption of the above PDLC films is in the range of 5 W m^{-2}, if powered with a line frequency of 50 Hz; at lower frequencies (e.g. 20 Hz) the power consumption can be reduced to about 2.5 W m^{-2} without lowering the change in transmittance significantly.

1. Introduction

Transparent insulation (TI) technology [1] is a promising instrument to minimize energy consumption for heating of residential buildings. To prevent overheating of the massive walls solar input has to be controlled reliably. Up to now mechanical shading devices such as reflective roller blinds have been used in TI systems.

Various non-mechanical shading devices are under investigation today:

- thermochromic materials [2, 3] form scattering particles when a switching temperature is surpassed,
- electrochromic films [4] absorb light when an electric voltage is applied,
- PDLC films [5] show a reduction in their light scattering efficiency when an electric field is applied.

Absorbing systems are not well suited for insolation control, because absorption of solar radiation within these materials may lead to overheating in the coloured state; this would require additional constructional precautions.

In this work we present recent results of our investigations into PDLC films, where light scattering is the predominant switching mechanism.

2. Specimens

PDLC films consist of μm-sized droplets of a nematic, birefringent liquid crystal embedded in a polymer matrix [5]. The ordinary refractive index n_o of the liquid crystal is chosen to match the refractive index n_m of the surrounding medium, its extraordinary refractive index n_e differs significantly. Without an external electric field the liquid crystal droplets are oriented randomly, the effective refractive index of the droplets differs considerably from the index of the polymer matrix. This leads to a strong scattering of incident light (figure 1(*a*)). If a sufficiently high electric field is applied, the liquid crystal molecules become aligned parallel to the field direction. The effective refractive index of an aligned droplet for normally incident light is the ordinary index of the liquid crystal, which is chosen to match the index of the matrix material. Thus light impinging in a near-normal direction onto the PDLC film remains nearly unscattered because of this index matching (figure 1(*b*)).

The method used for sample preparation was polymerization induced phase separation [6, 8]. The matrix material was the UV-curable polymer Norland optical adhesive 65 (NOA 65) [9], for liquid crystal the standard mixture E7 [7, 10] was used. The liquid crystal was dissolved in the uncured matrix material. Upon curing the solubility of the liquid crystal decreases, leading to a phase separation and formation of small liquid crystal droplets. Curing was performed with the radiation of a line focusing 500 W Hg-lamp. The curing rate can be controlled by the UV light intensity, i.e. by varying the distance between sample and light source or by the use of neutral density filters.

0022-3727/94/102145+07$19.50

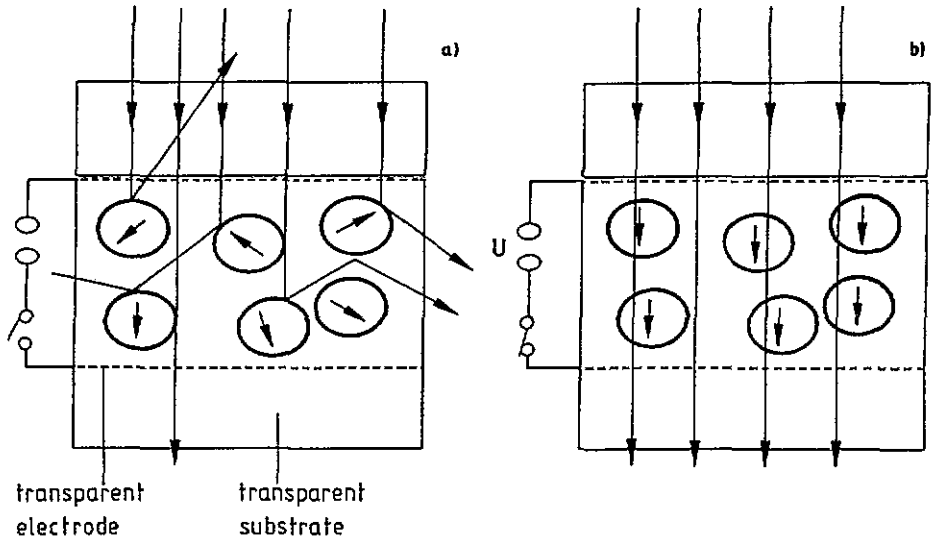

Figure 1. (*a*) Randomly oriented LC droplets lead to effective scattering in the unpowered state. (*b*) Matching the index of refraction in the powered state ensures a transparent layer.

PDLC films with a thickness of about 20 μm to 200 μm, sandwiched between two ITO-coated polyester foils, were produced. The film thickness was adjusted using spacers around the rims of the samples.

3. Theory

We used the Rayleigh–Debye approximation [11] to describe the scattering behaviour induced by small nematic droplets within PDLC films in the powered state. A nematic droplet is characterized by its radius R and its dielectric constants $\varepsilon_\perp = n_o^2$ and $\varepsilon_\parallel = n_e^2$; $\varepsilon_m = n_m^2$ is the dielectric constant of the surrounding medium. If the nematic droplets are located in a strong external electric field, which is oriented parallel to the direction of the incident light, the angular distribution $I_{s,\perp}$ for light polarized perpendicular to the scattering plane is given by [11]

$$\frac{I_{s,\perp}}{I_{0,\perp}} = \frac{R^2}{9r^2}(kR)^4 u^2(\zeta - \eta)^2 \qquad (1)$$

where r denotes the distance between the scattering volume and the detector and $k = 2\pi n_m/\lambda$ is the wavevector of the incident light with wavelength λ. $\zeta = (2\varepsilon_\perp + \varepsilon_\parallel)/(3\varepsilon_m) - 1$ and $\eta = (\varepsilon_\parallel - \varepsilon_\perp)/(3\varepsilon_m)$ describe the isotropic and the anisotropic part of the relative dielectric tensor. The relation

$$u = \frac{3}{(k_s R)^3}[\sin(k_s R) - k_s R\cos(k_s R)] \qquad (2)$$

is the well known Rayleigh–Debye scattering coefficient of a sphere with radius R [12], where $k_s = 2k\sin(\vartheta/2)$ is the momentum transfer.

The scattering of a particle collection with size distribution $v(R)$ and a scattering distribution $I(\vartheta, R)$ according to equation (1) can be calculated via [13]

$$I_j = I_{s,\perp}(\vartheta_j) = \int_0^\infty I(\vartheta_j, R)\frac{v(R)}{(4\pi/3)R^3}\mathrm{d}R \qquad (3)$$

where $v(R)\mathrm{d}R$ denotes the volume of particles within the radius interval R and $R + \mathrm{d}R$, thus $v(R)/(4\pi/3R^3)$ is the number of particles in this interval.

In order to derive an approximation for $v(R)$, the radial range from R_{min} to R_{max} is subdivided into n equally sized intervals, ranging from $R_i = R_{min} + (R_{max} - R_{min}(i-1)/n)$ to R_{i+1}. The radial distribution $v(R)$ is approximated by a constant value v_i in every interval. This simplifies equation (3) to

$$I_j = \sum_{i=1}^{N_s} v_i I_{i,j} \qquad I_{i,j} = \int_{R_i}^{R_{i+1}} \frac{1}{\frac{4\pi}{3}R^3} I(\vartheta_j, R)\mathrm{d}R. \qquad (4)$$

The parameters v_i describe the volume of droplets in the respective radial interval.

The solution of this linear, inhomogenous system of equations yields an approximation of the true particle size distribution. In equation (4) the line-index $j = 1 \ldots J$ symbolizes the intensity values measured at fixed scattering angles ϑ_j; the column-index $i = 1 \ldots N_s$ denotes the size intervals. The number of size intervals is smaller than the number of measured data points, thus an exact solution of equation (4) is impossible. The optimal parameters h_i are calculated using the single-value-decomposition method [14], which satisfies the least-squares condition.

To describe the radiative transport through a PDLC layer we used the radiative transport equation for non-emitting materials in the case of a azimuthally symmetric phase function $p(\vartheta', \vartheta)$ and normal incidence [15]

$$\cos\vartheta\frac{\mathrm{d}I(\tau,\vartheta)}{\mathrm{d}\tau} = I(\tau,\vartheta) - \frac{\omega_0}{2} \times \int_{-1}^{1} I(\tau,\vartheta')p(\vartheta',\vartheta)\mathrm{d}\cos\vartheta' - \frac{\omega_0}{4}F\mathrm{e}^{-\tau}p(0,\vartheta). \qquad (5)$$

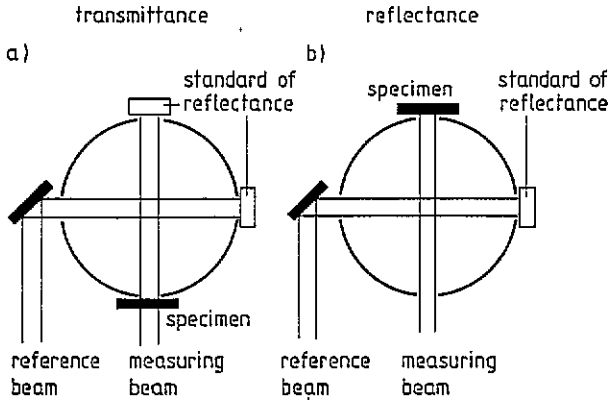

Figure 2. Integrating sphere arrangement for measurements of the directional-hemispherical transmittance (a) and reflectance (b).

where $p(\vartheta', \vartheta)$ describes the probability for light propagating in direction ϑ' to be scattered into direction ϑ. $I(\tau, \vartheta)$ denotes the radiation propagating in direction ϑ in an optical depth τ and $\omega = S/(S + A)$ is the albedo, where S and A are the scattering and absorption coefficients respectively. One also has to take into account the boundary conditions, which describe the angle-dependent reflection coefficients of the sample–air interface. We used a multi-flux calculation [3, 16] to solve equation (5).

4. Experimental set-up

The directional-hemispherical transmittance t_{dh} and reflectance r_{dh} of PDLC samples were measured using a UV/VIS/NIR double-beam spectrophotometer with an integrating sphere attachment [3]. This arrangement (figure 2) allows measurements in the spectral range from 250 nm to 2.5 μm.

In order to characterize the light scattering properties of PDLC films, differential light scattering measurements were performed using a polar nephelometer [3]. The sample is illuminated by a He–Ne laser beam at a wavelength λ of 633 nm, which is polarized perpendicularly to the scattering plane. The scattered intensity is measured as a function of the scattering angle.

In addition angular dependent directional-hemispherical measurements were performed at a fixed wavelength of 543 nm. The samples are mounted on the entrance port of a integrating sphere with a diameter of 30 cm. A He–Ne laser beam, expanded to a diameter of about 20 mm, illuminates the sample. The integrating sphere can be rotated around its entrance port to vary the angle of incidence of the laser beam (figure 3).

The samples were powered with an sinusoidal AC voltage. Normally the line frequency of 50 Hz was used, but some additional measurements were performed in the frequency range from about 10 Hz to 1000 Hz.

Voltage and current were measured simultaneously with an 12 bit AD converter at a sample rate of 8 kHz; the effective values and relative phase of voltage and

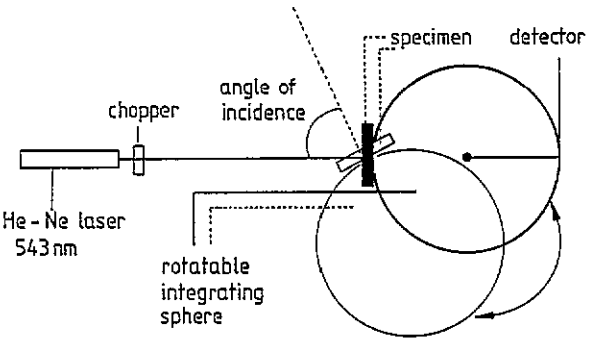

Figure 3. Integrating sphere arrangement for angular-dependent measurements.

current, the power consumption and the capacitance and resistance of the sample were calculated from these data. The measured values are I_j and U_j, measured at the time $t_j = j/f$ where f is the sampling frequency. The effective values I_{eff} and U_{eff} are calculated via

$$I_{\text{eff}} = \frac{1}{N}\sqrt{\sum_{j=1}^{N}(I_j)^2} \qquad \text{and} \qquad U_{\text{eff}} = \frac{1}{N}\sqrt{\sum_{j=1}^{N}(U_j)^2} \tag{6}$$

where N/f is a multiple of the cycle time of the applied voltage. The power consumption P can be calculated via

$$P = \frac{1}{N}\sum_{j=1}^{N} U_j I_j. \tag{7}$$

For sinusoidal voltages the power is defined by

$$P = U_{\text{eff}} I_{\text{eff}} \cos\varphi \tag{8}$$

where φ is the phase difference between voltage and current.

5. Measurements and discussion

5.1. Light scattering measurements

The light switching behaviour of PDLC films is induced by a change of the light scattering efficiency of the liquid crystal droplets, if an external electric voltage is applied. We used a polar nephelometer to investigate the light scattering distribution of PDLC specimens depending on the applied voltage. Figure 4 shows a typical scattering distribution of a 40 μm thick PDLC film for AC voltages at 50 Hz of 0, 40, 80, 120 and 140 V respectively.

Without an external electric field the scattering distribution is nearly isotropic. With increasing voltage the scattering distribution gets more and more forward peaked, while the total scattered intensity decreases. An increase in the voltage from 120 to 140 V no longer changes the scattering distribution significantly. In this case we can assume complete orientation of all liquid crystal molecules; droplet sizing using the histogram fit described in section 3 is possible. The good index matching between droplets and matrix in this case

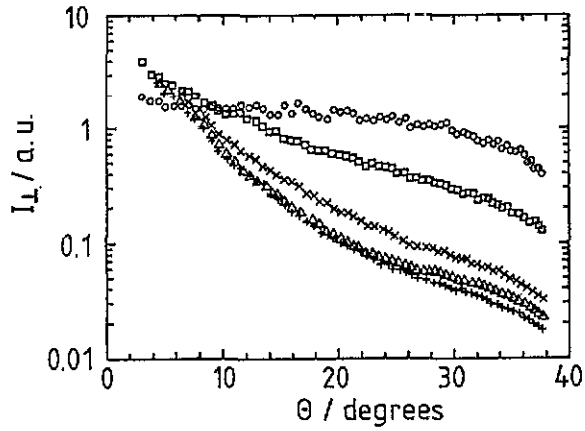

Figure 4. Scattering distribution of a 40 μm thick PDLC sample. Applied AC voltage is 0 V (○), 40 V (□), 80 V (×), 120 V (△) and 140 V (+).

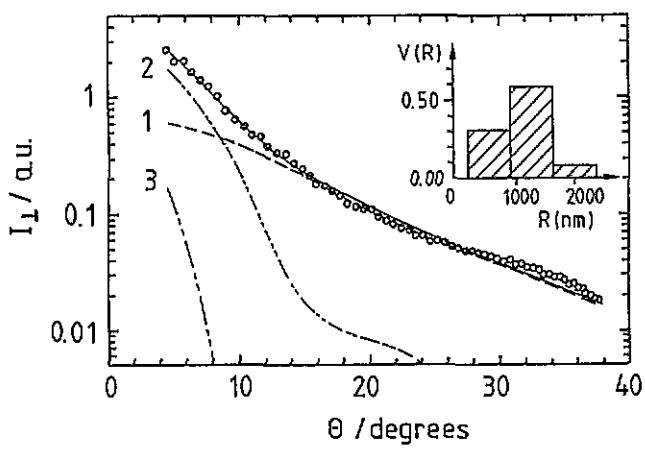

Figure 5. Measured scattering distribution for a voltage of 140 V (○); fit curve according to equation (4) (——); quotas of the size ranges: 200–900 nm (1), 900–1600 nm (2), 1600–2300 nm (3). In addition the relative volume $V(R)$ of droplets with radii in the three subintervals is plotted.

justifies the use of the Rayleigh–Debye approximation in equation (4).

Light microscopy allows to derive an upper limit of about 2 μm for the droplet radii. Taking this into account, we subdivided the size range from 200 nm to 2.3 μm into three equally sized intervals. A fit according to equation (4) yields the relative volumes of droplets in the three size ranges as shown in figure 5. Nearly all the liquid crystal volume is concentrated in droplets with radii below 1.6 μm. Adding a fourth interval with larger radii does not change the result; the contribution of particles with radii above 2.3 μm is zero within the error range. Figure 5 shows the measured scattering distribution at a voltage of 140 V, the fit curve and the contributions from the three particle sizes. The light scattering properties are dominated by the smallest droplets with radii below 0.9 μm, only at scattering angles below 12° is the contribution of larger droplets noticeable.

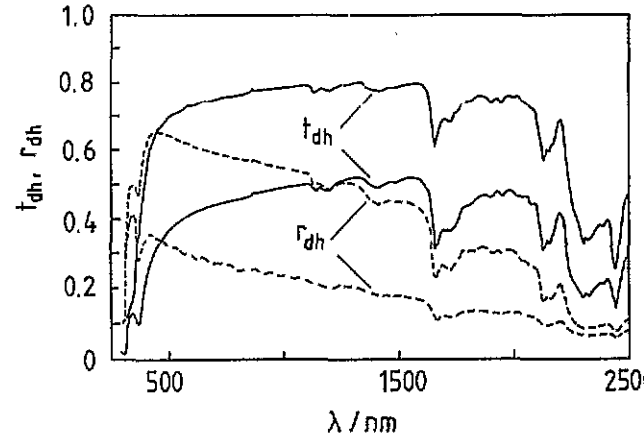

Figure 6. Directional-hemispherical transmittance t_{dh} (——) and reflectance r_{dh} (– – –) of a 150 μm thick PDLC sample versus wavelength in the scattering and transmitting state.

5.2. Directional-hemispherical measurements

The applicability of shading devices depends on their radiation transport properties. Important in this respect are the solar-averaged transmittance $\bar{t}_{dh,solar}$ and reflectance $\bar{r}_{dh,solar}$. These quantities are calculated by averaging the spectral hemispherical data weighted with an AM 1.5 solar spectrum [17], this means a solar spectrum after penetration of 1.5 atmospheric thicknesses. Figure 6 shows typical transmission and reflection spectra of a PDLC specimen in the scattering and transparent state. In the transparent state the transmittance is nearly wavelength independent except for some absorption bands of the matrix material and the polyester foils in the near IR and in the UV region. Switching to the scattering state reduces the transmittance by about 30% in the visible and NIR spectral region; the reflection increases by the same amount. This proves that the light switching is only due to scattering; the absorption of the PDLC film is negligible in the spectral region from 400 to 1500 nm in both the transparent and the scattering state.

In order to optimize the light switching behaviour of the PDLC layers we varied different preparation parameters, namely the film thickness, the concentration of the liquid crystal in the matrix material and the curing rate (the UV light intensity during curing of the matrix material).

The influence of the sample thickness on the transmission reduction was measured for two PDLC samples (A and B); all other preparation parameters were left unchanged. While the film thickness increased from 60 to 150 μm, the transmission reduction of set (A) showed only a small increase from 26 ± 2% to 30±2%; set (B) showed a similar increase from 21±2% (d = 40 μm) to 23 ± 2% (d = 120 μm).

With increasing film thickness the transmittance in the off-state decreases. Unfortunately a decrease of the transmittance in the on state was also observed; the samples are not perfectly transparent, but show some scattering even when a voltage is applied. This effect is caused by a non-optimal index matching between the ordinary refractive index of the liquid crystal and

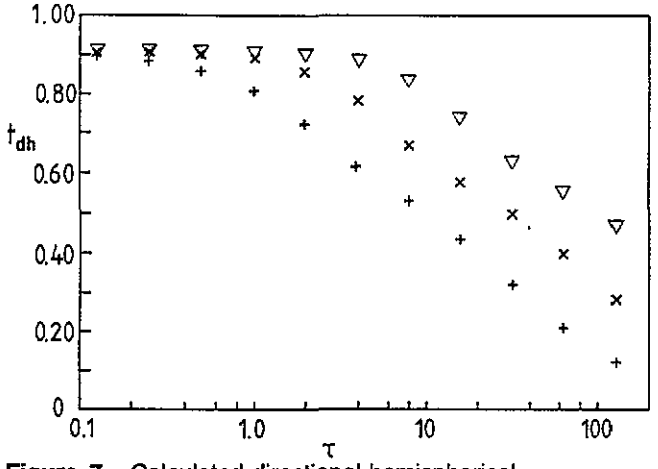

Figure 7. Calculated directional-hemispherical transmittance t_{dh} depending on the optical thickness τ; parameter is the size parameter $X = 2\pi n_m R/\lambda$: $X = 3.5$ (+), $X = 7.0$ (×), $X = 14$ (▽).

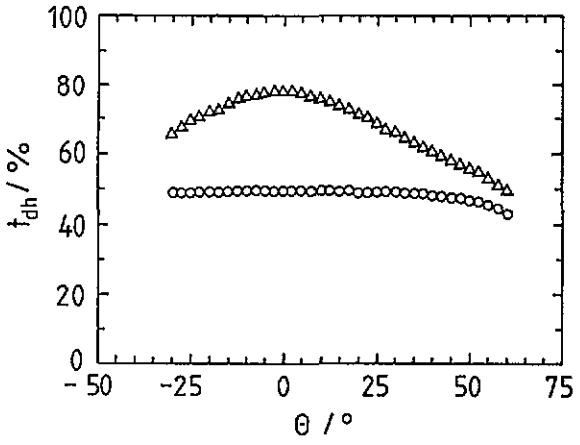

Figure 8. Directional-hemispherical transmittance of a 100 μm PDLC film dependent on angle of incidence at a wavelength of 543 nm (○) off state; (△) on state.

the matrix material and additionally by the droplets not being perfectly aligned. This holds even in the case if significantly overdriven samples. The ratio of the extinction coefficients of the off and on states depends on the used materials and preparation parameters; it is independent of the specimen thickness.

Radiative transport calculations (figure 7) allow us to determine the diffuse transmittance of a layer depending on its scattering distribution and optical thickness $\tau = Sd$, where S is the scattering coefficient and d the geometrical thickness of the sample. Clearly visible is a decrease in t_{dh} with increasing τ ($t_{dh} \propto 1/\tau$ for big τ). Increasing the film thickness increases the optical thickness in the on and off states by the same factor. Thus the transmittance in both states decreases by the same amount when the initial optical thickness in the on state was greater than τ_c. This leaves the transmission reduction practically unchanged.

The concentration of the liquid crystal in the matrix material changes the total volume of the liquid crystal droplets, thus affecting the average droplet size and the droplet number density in the PDLC layer. For the materials used a mass ratio of 1.2 g (LC) per 1 g (NOA 65) performed best. Using 0.8 g or 1.6 g of the liquid crystal per 1 g NOA 65, the transmission reduction decreased; for 0.4 g LC per 1 g NOA 65 no opaque specimen could be prepared at room temperature.

The curing rate of the specimen is controlled via the intensity of the UV light. Blocking 50%, 90% and 99% of the UV light using neutral density filters decreased the transmission reduction from about 23% to 16%, 12% and 6%, respectively.

To study the effect of greater curing intensity, the distance between lamp and specimen was reduced from 320 mm to 80 mm and finally to 40 mm. For both sets of PDLC specimens (LC/NOA 65 = 0.8 and 1.2) the highest transmission reduction was obtained at a distance of 80 mm.

The change in the liquid crystal concentration changes the total droplet volume in the PDLC layer. One should take into account the fact that part of the liquid crystal is still solved in the cured matrix material, as can be seen in the case of the 0.4/1-mixture, where no droplets are formed during curing. This increase of the droplet volume explains the rise of the transmission reduction up to the mass ratio of 1.2/1. Further increase in the liquid crystal concentration also causes a greater average droplet size. This leads to a more forward peaked scattering distribution and larger diffuse transmittance; thus it reduces the shading performance of the film.

A faster curing rate yields a smaller droplet size [6]. Both the scattering coefficient and the scattering distribution depend strongly on the particle size. Very small droplets show an isotropic scattering distribution, but their total scattering coefficient decreases $\propto R^6$ (Rayleigh scattering), while the scattering distribution of large particles is strongly forward peaked, thus increasing the hemispherical transmittance.

Another important parameter is the angular dependent directional-hemispherical transmittance $t_{dh}(\vartheta)$ of PDLC samples. The angle of incidence in practical applications can be expected to differ significantly from 90° during days and seasons. Figure 8 shows $t_{dh}(\vartheta)$ of a 100 μm thick specimen at a wavelength of 543 nm, which is near the maximum of the solar spectrum, in the on and off state. In the off state $t_{dh}(\vartheta)$ is nearly independent of the angle of incidence. Upon switching the directional-hemispherical transmittance has a maximum at normal incidence. For increasing angle of incidence the effective index of refraction of the droplets rises because of the increasing influence of the extraordinary refractive index; the degree of index matching and thus the transparency of the layer decrease with increasing angle of incidence.

5.3. Electrical properties of PDLC layers

The power consumption of PDLC layers is a very important parameter for their applicability as shading devices in solar architecture. In order to determine the electrical properties of the PDLC specimens, we

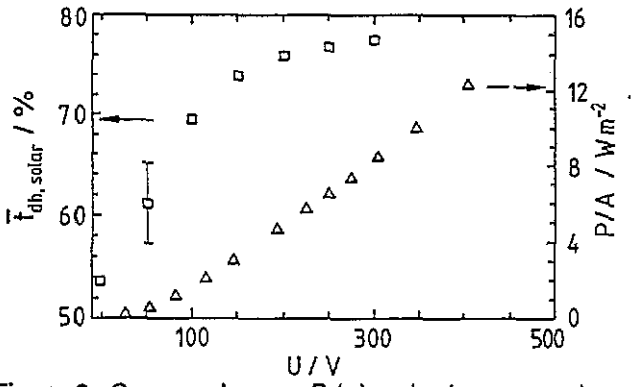

Figure 9. Consumed power P (△) and solar-averaged transmittance $\bar{t}_{dh,solar}$ (□) versus applied voltage U of a typical PDLC film.

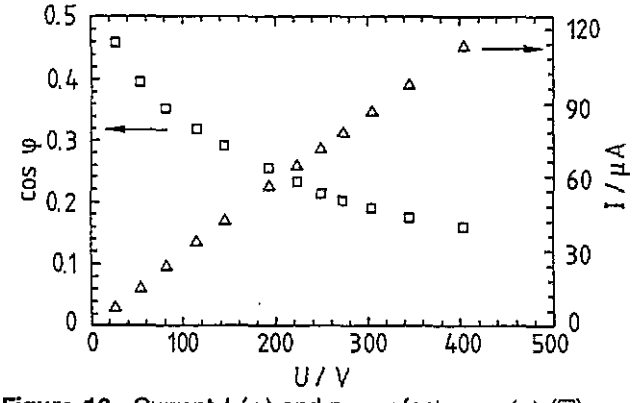

Figure 10. Current I (△) and power factor cos(φ) (□) depending on the applied voltage U for the sample used in figure 9.

measured the power consumption depending on voltage and frequency of the applied sinusoidal voltage.

Figure 9 shows a plot of the power consumption per unit area of a typical PDLC specimen versus applied voltage. In addition the solar-averaged transmittance to show the optical switching is plotted. A voltage of 200 V yields a transmission reduction of about 25% at a power consumption of about 5 W m^{-2}. Increasing the voltage to 300 V increases the transmission reduction by only 1.3%, while the power consumption nearly doubles. The power consumption is not proportional to the square of the applied voltage; this means that the electrical impedance of the layer depends on the applied voltage. This can also be seen in figure 10, which shows the power factor cos φ depending on the applied voltage. Clearly visible is a decrease of cos φ with increasing voltage.

In addition the power consumption depending on the frequency of the applied sinusoidal voltage was investigated. Figure 11 shows the wattage and cos φ of a 40 μm thick PDLC specimen at a voltage of 80 V. One observes a linear increase of the power consumption with increasing frequency; cos φ slightly decreases with increasing frequency.

The dependence of the specimens transmittance on the frequency of the applied voltage is shown in table 1. In the frequency range 10–1000 Hz the solar averaged transmittance changes by only about 1%; the transmittance increases monotonically with increasing

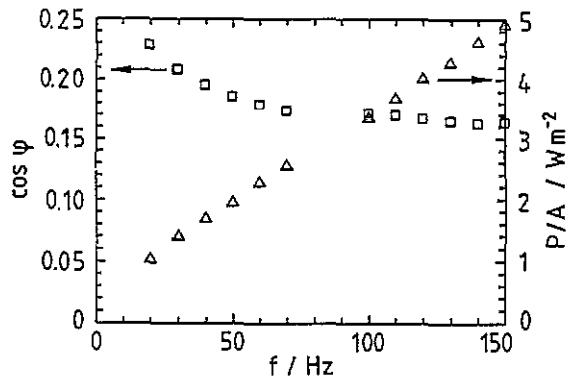

Figure 11. Power consumption P (△) as a function of the frequency f at an applied voltage of 80 V. In addition the power factor cos(φ) is plotted (□).

Table 1. Solar averaged transmittance of a PDLC sample versus frequency of the applied voltage.

f (Hz)	10	25	50	100	250	1000
$t_{dh,solar}$ ($U = 25$ V) (%)	—	72.5	72.7	72.9	—	73.6
$t_{dh,solar}$ ($U = 50$ V) (%)	78.0	78.1	78.2	78.6	78.8	79.2

frequency. The influence of the shape of the voltage on the transmittance was also investigated. A specimen powered with sine, triangle and square waves with the same effective voltage at a frequency of 50 Hz shows no difference in the transmittance within the experimental error of the used spectrophotometer.

A straightforward electric model of a PDLC film is a parallel connection of a capacitor and an ohmic resistance. The former represents the PDLC material as dielectric and the transparent conducting films as electrodes, the latter the non-vanishing conductivity of the PDLC material. However, this simple model cannot describe the measured voltage and frequency dependent electrical properties of PDLC specimens, because it predicts a frequency independent power consumption which is proportional to the square of the applied voltage.

The first correlation $C(U)$ (figure 12) derived from the experimental data shows an increase in the capacity with increasing voltage until the switching voltage is surpassed. This behaviour can be explained by the electrical anisotropy of the liquid crystal droplets in the film. If the voltage rises, more and more liquid crystal molecules align parallel to the applied electric field; therefore the effective dielectric constant and thus the capacity of the layer rise until all droplets are fully aligned.

The frequency dependence of the power consumption of the switching system can be explained by a modified model. The orientation of the liquid crystal droplets consumes a certain amount of energy in every cycle. This means that the power consumption is proportional to the number of cycles per time interval, i.e. the frequency f of the applied voltage. There is an

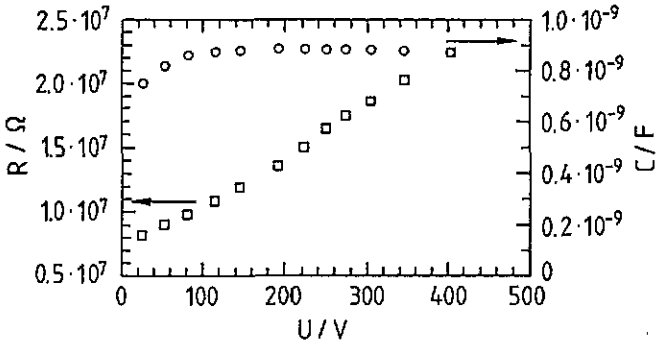

Figure 12. Resistance R (□) and capacity C (○) of the sample used in figure 9 depending on the applied voltage U.

additional small, frequency independent contribution, which can be found from an extrapolation $f \rightarrow 0$. The resulting ohmic resistance, which is approximately 500 k Ω m^2, is responsible for this offset.

An important outcome is the possibility to reduce the power consumption of a PDLC film by nearly 50% without changing the optical properties simply by reducing the frequency of the driving voltage from 50 to 20 Hz.

6. Conclusions

The investigated PDLC films allow a transmission reduction of about 30% in the solar spectral range; they consume a power of about 5 W m^{-2} for switching in the transparent state. This change in transmission is caused by light scattering by liquid crystal droplets with radii below 1 μm. For many shading applications a higher transmission reduction is necessary. One possibility is the use of liquid crystal mixtures with higher birefringence to increase the scattering coefficient in the off-state, another is the optimization of the index matching to obtain more transparent samples in the on state.

The description of the electrical properties of PDLC films has not been satisfactory up to now; further investigations are necessary in order to minimize the power consumption in the on state. The strong dependence of the power consumption on the frequency of the applied voltage yields some potential with respect to that goal.

Acknowledgments

This work was supported by the german BMFT. We are indebted to Merck Ltd, Darmstadt for providing liquid crystal samples.

References

[1] Goetzberger A and Wittwer V 1986 *Aerogels (Springer Proc. in Physics 6)* ed J Fricke (Heidelberg: Springer)
[2] Beck A 1992 Struktur- und Strahlungstransport-Untersuchungen an thermochromen Gelen *PhD thesis* University of Würzburg, Germany
[3] Beck A, Körner W, Hoffmann T and Fricke J 1992 Light-scattering investigations of thermochromic gels *Appl. Opt.* **31** 3533–9
[4] Bange K and Gambke T 1990 Electrochromic materials for optical switching devices *Adv. Mater.* **2** 1
[5] Doane J W, 1991 Polymer dispersed liquid crystal displays *Liquid Crystals, Applications and Uses* ed B Bahadur (Singapore: World Scientific) p 361
[6] Jubb R and Finkenzeller U 1991 *Creating Experimental NCAP/PDLC Devices: A Compilation of Basic Instructions* E Merck Proprietary Information, Darmstadt, Germany
[7] Coates D, Greenfield S, Sage I C and Smith G 1990 Liquid crystal mixtures for polymer matrix displays *SPIE Proc.* **1257** 37–45
[8] West J L 1988 Phase separation of liquid crystals in polymers *Mol. Cryst. Liq. Cryst.* **157** 427–41
[9] 1991 *Norland Optik-Kleber Data Sheet* Lubrical GmbH, Brombachtal, Germany
[10] 1992 *Liquid Crystal E7 Data Sheet* Merck House, Poole, Dorset
[11] Žumer S and Doane J W 1986 Light scattering from a small nematic droplet *Phys. Rev.* A **34** 3373
[12] Kerker M 1969 *The Scattering of Light* (New York: Academic)
[13] Dave J V 1971 Determination of size distribution of spherical polydispersions using scattering radiation data *Appl. Opt.* **10** 9
[14] Press W, Flannery B, Teukolsky S and Vetterling W 1989 *Numerical Recipes in Pascal* (Cambridge: Cambridge University Press)
[15] Chandrasekhar S 1960 *Radiative Transfer* (New York: Dover)
[16] Watermann P C 1981 Matrix-exponential description of radiative transfer *J. Opt. Soc. Am.* **71** 410–22
[17] Bird R E, Hustrom R L and Lewis L J 1983 Terrestrial solar spectral data sets *J. Sol. Energy* **30** 563–7